Effect of Molecular Orientation on Monolayer and Multilayer Formations of Fluorocarbon Alcohol and Fluorocarbon−α,ω−diol Mixture at the Hexane/water Interface

ARTICLE *in* THE JOURNAL OF PHYSICAL CHEMISTRY B · OCTOBER 2014

Impact Factor: 3.3 · DOI: 10.1021/jp507049z · Source: PubMed

8 AUTHORS, INCLUDING:

Ryushi Fukuhara
Kyushu University
1 PUBLICATION **2** CITATIONS
SEE PROFILE

Hiroki Matsubara
Kyushu University
84 PUBLICATIONS **693** CITATIONS
SEE PROFILE

Makoto Aratono
Kyushu University
206 PUBLICATIONS **3,127** CITATIONS
SEE PROFILE

Takanori Takiue
Kyushu University
111 PUBLICATIONS **1,050** CITATIONS
SEE PROFILE

THE JOURNAL OF PHYSICAL CHEMISTRY B

Article

pubs.acs.org/JPCB

Effect of Molecular Orientation on Monolayer and Multilayer Formations of Fluorocarbon Alcohol and Fluorocarbon-α,ω-diol Mixture at the Hexane/water Interface

Ryushi Fukuhara,[†] Hajime Tanida,[‡] Kiyofumi Nitta,[‡] Toshiaki Ina,[‡] Tomoya Uruga,[‡] Hiroki Matsubara,[†] Makoto Aratono,[†] and Takanori Takiue*,[†]

[†]Department of Chemistry, Faculty of Sciences, Kyushu University, Fukuoka 812-8581, Japan

[‡]Japan Synchrotron Radiation Research Institute, Hyogo 678-5198, Japan

ABSTRACT: The effect of molecular orientation on the miscibility and structure of the adsorbed film of the 1*H*,1*H*,10*H*,10*H*-perfluorodecane-1,10-diol (FC_{10}diol)−1*H*,1*H*,2*H*,2*H*-perfluorodecanol ($FC_{10}OH$) mixture at the hexane/water interface were examined by interfacial tension and X-ray reflectivity measurements. The interfacial tension and X-ray reflectivity at the hexane solution/water interface were measured as a function of total molality m and composition of $FC_{10}OH$ in the mixture X_2 under atmospheric pressure at 298.15 K. The interfacial pressure vs mean area per molecule curves showed that two kinds of condensed monolayers (C1 and C2) and multilayer (M) states appeared depending on m and X_2. In the pure component systems, it was found that $FC_{10}OH$ forms condensed monolayer in which the molecules orient almost normally to the interface, and FC_{10}diol orients parallel and is densely packed in the condensed monolayer and then piles spontaneously to form multilayer. In the mixed system, the phase diagram of adsorption indicated that $FC_{10}OH$ molecules are richer in C2 than in C1 state. The X-ray reflectivity measurements manifest that the condensed monolayer below X_2 = 0.985 is heterogeneous in which the normal- and parallel-oriented domains coexist at the interface (C1 state), and that above X_2 = 0.985 seems to be homogeneous with normal molecular orientation (C2 state). The structure of M state depends on those of condensed monolayers, on which the molecules pile spontaneously. The heterogeneous structure in C1 state is compared to that previously observed in the mixed system of FC_{10}diol−$FC_{12}OH$ (1*H*,1*H*,2*H*,2*H*-perfluorododecanol), where $FC_{12}OH$ has longer fluorocarbon chain length than $FC_{10}OH$ and is discussed in terms of domain line tension.

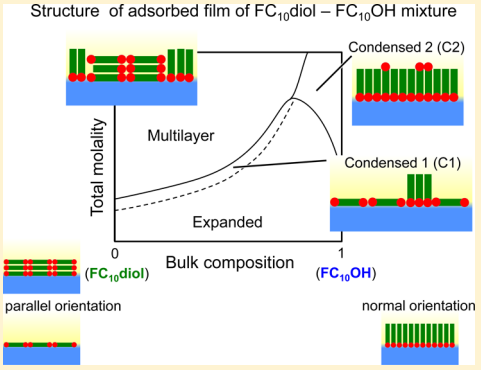

INTRODUCTION

The structure and property of interfacial films at soft interfaces including gas/liquid and liquid/liquid interfaces depend on the chemical structure of molecules, the mutual interaction between film forming molecules, and so on. The self-organization of molecules at the soft interfaces is of great importance because it is closely related to the appearance of new property of soft matters such as foam, emulsion, and biological membrane. Thus, the study on the molecular organization at the interface is essential to understand the structure−function relation of soft matters.

Many researchers have explored the state of interfacial films of not only single component but also plural component systems from the macroscopic and microscopic viewpoints and discussed the phase transition, the miscibility of molecules, and the microphase separation (domain formation) in the interfacial films.[1−10] For example, in the case of the Langmuir film composed of phospholipids and cholesterol, it was found that the lateral phase separation, in which two liquid like phospholipid-rich and cholesterol-rich phases coexist with each other, takes place depending on the molar ratio of lipids and cholesterol.[1−3] In the cholesterol-rich phase, cholesterol and phospholipids interact effectively with each other and form well-ordered film structure. Similar two-dimensional liquid−liquid phase separation was also observed in the phospholipid bilayer system,[11−13] and these heterogeneous structures are considered to be the fundamental framework of the biomembrane "raft" in which the important intercellular processes such as molecular recognition and transfer of molecules and ions are carried out.[14−16]

In the course of our systematic studies on the adsorption of molecules at the air/water and oil/water interfaces, the mixing of molecules in the adsorbed film was examined by constructing the phase diagram of adsorption (PDA) from thermodynamic analysis of interfacial tension data and by evaluating the electron density profile from X-ray reflectivity measurement. Among others, in our previous study on the adsorbed films of 1-icosanol ($C_{20}OH$)−1*H*,1*H*,2*H*,2*H*-perfluorodecanol

Received: July 15, 2014
Revised: October 2, 2014
Published: October 3, 2014

($FC_{10}OH$) mixture at the hexane/water interface,[7−10] the PDA indicated that $C_{20}OH$ and $FC_{10}OH$ molecules are miscible in the expanded state, whereas they are practically immiscible in the condensed state. The mixing of both alcohols in the expanded state accompanied a large positive excess Gibbs energy of adsorption due to weaker molecular interaction between fluorocarbon (FC) and hydrocarbon (HC) chains than between the same ones. Furthermore, it was found that $FC_{10}OH$ molecules form a condensed phase domain surrounded by a low density gaseous phase in the expanded state, and the two kinds of domains, $FC_{10}OH$ condensed and $C_{20}OH$ condensed domains, coexist in the temperature range close to the phase transition between the $FC_{10}OH$ condensed and $C_{20}OH$ condensed states.

The molecular orientation affects appreciably the molecular miscibility in the adsorbed film. For example, the study on the miscibility of 1*H*,1*H*-perfluorononanol ($FDFC_9OH$) and its ω-hydrogenated analogue, 1*H*,1*H*,9*H*-perfluorononanol ($HDFC_9OH$), which tilts around 15° from interface normal,[17,18] in the adsorbed film at the hexane/water interface showed that the excess Gibbs energy of adsorption is negative in the gaseous state, whereas it is positive in the condensed state.[19] This was reasonably explained by the balance of two effects: (1) reduction of repulsive interaction between the terminal dipoles (ω-dipole) aligning parallel in the adsorbed film and (2) the loss of dispersion interaction between hydrophobic chains due to the fact that oblique-oriented $HDFC_9OH$ mix with normal-oriented $FDFC_9OH$ at the interface.

"Bolaform" amphiphiles, which has two hydrophilic groups at both ends of hydrophobic chain, with HC chain are known as the molecules taking an "arch-like" conformation at the air/water interface because of flexible nature of HC chain.[20−22] Their two head groups are anchored into water phase and the HC chain is bent forward to air phase to avoid the contact of HC chain with water. On the other hand, it was highly expected that the FC-α,ω-diol "FC_ndiol (n = 8 and 10)", which has two hydroxyl groups at both ends of FC chain, orient parallel to the air/water and hexane/water interfaces due to the rigid nature of FC chains.[23−25] Furthermore, it was found that FC_ndiol molecules form not only monolayers but also multilayers with parallel orientation depending on temperature, pressure, and concentration of the solution.

In this paper, we aim at discussing the effect of molecular orientation on the molecular miscibility and structure of the adsorbed film. Thus, we employed two surface-active substances, $FC_{10}OH$ and 1*H*,1*H*,10*H*,10*H*-perfluorodecane-1,10-diol (FC_{10}diol), which adsorb at the hexane/water interface with different molecular orientations. The interfacial tension and X-ray reflectivity measurements showed that two kinds of condensed monolayer (C1 and C2) and multilayer (M) states appeared depending on the bulk composition and the total concentration of the mixture. It was concluded that both $FC_{10}OH$ and FC_{10}diol molecules are mixed with normal orientation in the C2 state, whereas the normal- and parallel-oriented domains coexist in the C1 state. Furthermore, FC_{10}diol molecules preferentially pile on the C1 and C2 states to form M state.

EXPERIMENTAL METHODS

Materials. 1*H*,1*H*,2*H*,2*H*-Perfluorodecanol ($FC_{10}OH$) and 1*H*,1*H*,10*H*,10*H*-perfluorodecane-1,10-diol (FC_{10}diol) purchased from Azmax Co., Ltd. were purified by recrystallization once from hexane and twice from chloroform solutions, respectively. Their purities were checked by observing no time dependence of the interfacial tension between hexane solution and water and by the liquid−gas chromatography; 99.8% for FC10OH and 99.9% for FC10diol.

Hexane (Aldrich Chemical Co. Inc.) was distilled once and water was produced by Millipore Milli-Q system.

Interfacial Tensiometry. The interfacial tension γ of the hexane solutions of FC_{10}diol−$FC_{10}OH$ mixture against water was measured as a function of the total molality m and the bulk composition of $FC_{10}OH$ X_2 in the mixture defined respectively by

$$m = m_1 + m_2 \tag{1}$$

and

$$X_2 = m_2/m \tag{2}$$

at 298.15 K under atmospheric pressure by the pendant drop method,[26] where m_1 and m_2 are respectively the molalities of FC_{10}diol and $FC_{10}OH$. For the calculation of γ values, the densities of pure hexane and water were used instead of those of the hexane solution and water in equilibrium with each other, because the concentrations of solutions were sufficiently low and mutual solubility between hexane solution and water is negligibly small. The experimental error of γ value was estimated within ±0.05 mN m^{-1}.

X-ray Reflection. X-ray reflectivity from the hexane solution/water interface was measured at the beamline BL37XU in SPring-8 by using a liquid surface spectrometer.[27] An X-ray beam introduced into the experimental hutch is diffracted by a Ge(111) crystal to select the energy (25 keV) and adjust the incident angle of the beam. A slit placed in front of the sample cell determines the beam size. The slit gaps were 10 μm in vertical and 200 μm in horizontal. The footprint on the surface is around 2 cm along the beam path. A N_2 gas ion chamber was put between the slit and the sample cell to measure the incident X-ray flux. The intensity of reflected beam was detected by two-dimensional detector (PILATUS) equipped with a copper−aluminum absorber to reduce the X-ray photons to optimum amounts.

The cell is made of stainless steel and equipped with Mylar windows. In specular reflection condition, the scattering vector $\mathbf{Q} = \mathbf{k}_{scat} - \mathbf{k}_{in}$ is only in normal to the interface (z-direction) and given by $Q_z = (4\pi/\lambda)\sin\alpha$, where λ (=0.496 Å) is the X-ray wavelength used in the present study, and α is the incident angle. The measurement was carried out at given molality and bulk composition under atmospheric pressure. Temperature was controlled at 298.15 ± 0.1 K by the Peltier device equipped to the cell.

X-ray reflectivity $R(Q_z)$ measured as a function of the scattering vector Q_z can be interpreted to yield the electron density profile normal to the interface. Under the first Born approximation, $R(Q_z)$ is given by[28,29]

$$\frac{R(Q_z)}{R_F(Q_z)} \cong \left| \frac{1}{\rho_w - \rho_h} \int \frac{d\langle\rho(z)\rangle}{dz} \exp(-iQ_z z)\, dz \right|^2 \tag{3}$$

where $\langle\rho(z)\rangle$ is the electron density profile averaged over the interfacial plane along with z-direction which is normal to the interface, ρ_w and ρ_h are respectively the electron densities of bulk water and hexane phases, and $R_F(Q_z)$ is Fresnel reflectivity for an ideally smooth interface described by[29,30]

$$R_F(Q_z) \approx \left| \frac{Q_z - Q_z^T}{Q_z + Q_z^T} \right|^2 \quad (4)$$

where Q_z^T is the z-component of the scattering vector with respect to the lower phase given by

$$Q_z^T \approx \sqrt{Q_z^2 - Q_c^2} \quad (5)$$

Here, the total reflection of X-ray from the lower phase occurs for $Q_z < Q_c$, where the scatter vector at critical angle Q_c is calculated by using the difference of bulk densities $\Delta\rho$ ($=\rho_w - \rho_h$) as

$$Q_c \approx 4\sqrt{\pi \Delta\rho r_e} \quad (6)$$

where r_e is the classical electron radius r_e = 2.818 fm.

The adsorbed films at the hexane/water interface are modeled by n slabs. Interfaces at the top and bottom of each slab will be fluctuated with thermally exited capillary waves,[31,32] which broadens the interface with an error function of interfacial roughness σ. Thus, the electron density for n-slab model is given by

$$\langle \rho(z) \rangle = \frac{1}{2}(\rho_w + \rho_h) + \frac{1}{2} \sum_n^{i=0} (\rho_i - \rho_{i+1}) \operatorname{erf}\left(\frac{z + \sum_{j=0}^{i} L_j}{\sqrt{2}\sigma} \right) \quad (7)$$

with

$$\operatorname{erf}(z) = \frac{2}{\sqrt{\pi}} \int_z^0 e^{-t^2} dt \quad (8)$$

where ρ_i and L_i are the electron density and thickness of slab i, respectively.

The interfacial roughness σ is usually considered to be the combination of two different contributions: the intrinsic profile width σ_0 and the resolution dependent capillary wave contribution σ_{cap}. In the hybrid model, the interfacial roughness is described as $\sigma^2 = \sigma_0^2 + \sigma_{cap}^2$. The Buff, Lovett, and Stillinger capillary wave theory[31] predicts σ_{cap} as

$$\sigma_{cap}^2 = \frac{k_B T}{2\pi} \int_{q_{max}}^{q_{min}} \frac{q}{\gamma q^2 + \Delta d_m g} dq \approx \frac{k_B T}{2\pi\gamma} \ln\left(\frac{q_{max}}{q_{min}} \right) \quad (9)$$

where γ is the interfacial tension of the hexane/water interface, $k_B T$ is the Boltzmann constant times the temperature, Δd_m ($=d_w - d_h$) is the difference of mass densities between two bulk phases, g is the gravitational acceleration, q_{min} ($=(2\pi/\lambda)\Delta\beta \sin\alpha$) with the angular acceptance of the detector $\Delta\beta = 6.37 \times 10^{-4}$, and $\Delta d_m g \ll q_{min}^2$. q is the in-plane wave vector of the capillary waves. The limit, q_{max}, is determined by the cutoff for the smallest wavelength of capillary waves that the interface can support. We have chosen $q_{max} = 2\pi/l$ Å^{-1} where l is an approximate size of hexane molecule.

In the case of laterally heterogeneous film consisting of domains, another analysis of $R(Q_z)$ can be applied. On the one hand, if the spatial coherent length of the X-ray in the plane of the interface is much larger than the domain size, the X-rays reflected from domains 1 and 2 interfere nearly coherently. In this case, the amplitudes of reflected electromagnetic fields should be added, and then, the coherent X-ray reflectivity $R_{coh}(Q_z)$ is given by[10]

$$R_{coh}(Q_z) = |C r_1(Q_z) + (1 - C) r_2(Q_z)|^2 \quad (10)$$

where r_1 and r_2 are the reflection amplitudes of the coexisting domains 1 and 2, respectively, and C is the area coverage of domain 2 in the adsorbed film. On the other hand, if the domains are much larger than the coherent length of X-ray, the interference between neighboring phases is incoherent. Then, the incoherent reflectivity $R_{inc}(Q_z)$ is provided by

$$R_{inc}(Q_z) = C R_1(Q_z) + (1 - C) R_2(Q_z) \quad (11)$$

where $R_1(Q_z)$ and $R_2(Q_z)$ are the X-ray reflectivity from domains 1 and 2, respectively.

RESULTS AND DISCUSSION

Interfacial Tension. In Figure 1 are shown the equilibrium interfacial tension γ vs total molality m curves at constant bulk composition X_2 in the FC_{10}diol–FC_{10}OH mixed system. The γ vs m curves below X_2 = 0.8 are magnified in the inset. The γ values decrease gradually with increasing m, and the γ vs m curves have one or two break points due to the phase transition in the adsorbed film. The curves below X_2 = 0.98 (curve 10) have a break point, and their shapes change regularly from that of the pure FC_{10}diol system (curve 1) with increasing X_2. The curves above X_2 = 0.99 (curve 13) also show a break which changes gradually from that observed in pure FC_{10}OH system (curve 15). At X_2 = 0.982 and 0.985 (curves 11 and 12), the curves have two break points at m = 7.5 and 7.85 mmol kg^{-1} at X_2 = 0.982 and m = 7.45 and 9.75 mmol kg^{-1} at X_2 = 0.985 (indicated by arrows).

The interfacial tension γ^{eq} and the corresponding total molality m^{eq} at the phase transition points are plotted against X_2 (filled circles) in Figures 2 and 3, respectively. Three kinds of curves originated from the three types of phase transitions meet at m^{eq} = 7.6 mmol kg^{-1}, γ^{eq} = 29.8 mN m^{-1}, and X_2 = 0.981, indicating that in the FC_{10}diol–FC_{10}OH system, at least three different states appear depending on m and X_2.

Here let us briefly introduce the thermodynamic equations for analyzing the interfacial tension data. The total differential of γ for binary nonionic–nonionic mixtures is expressed as a function of temperature T, pressure p, and the chemical potential of solute i, μ_i (i = 1, 2) by[33,34]

$$d\gamma = -s^H dT + v^H dp - \Gamma_1^H d\mu_1 - \Gamma_2^H d\mu_2 \quad (12)$$

Assuming that the hexane solution is ideally dilute and substituting the total differential of chemical potential of each component into eq 12, we have

$$d\gamma = -\Delta s\, dT + \Delta v\, dp - \Gamma^H (RT/m)\, dm - \Gamma^H (RT/X_1 X_2)(X_2^H - X_2)\, dX_2 \quad (13)$$

where Δs and Δv are respectively the entropy and volume changes associated with adsorption, Γ^H is the total interfacial density, and X_2^H is the composition of FC_{10}OH in the adsorbed film defined respectively by

$$\Delta y = y^H - \Gamma_1^H y_1^O - \Gamma_2^H y_2^O \qquad (y = s, v) \quad (14)$$

$$\Gamma^H = \Gamma_1^H + \Gamma_2^H \quad (15)$$

and

$$X_2^H = \Gamma_2^H / \Gamma^H \quad (16)$$

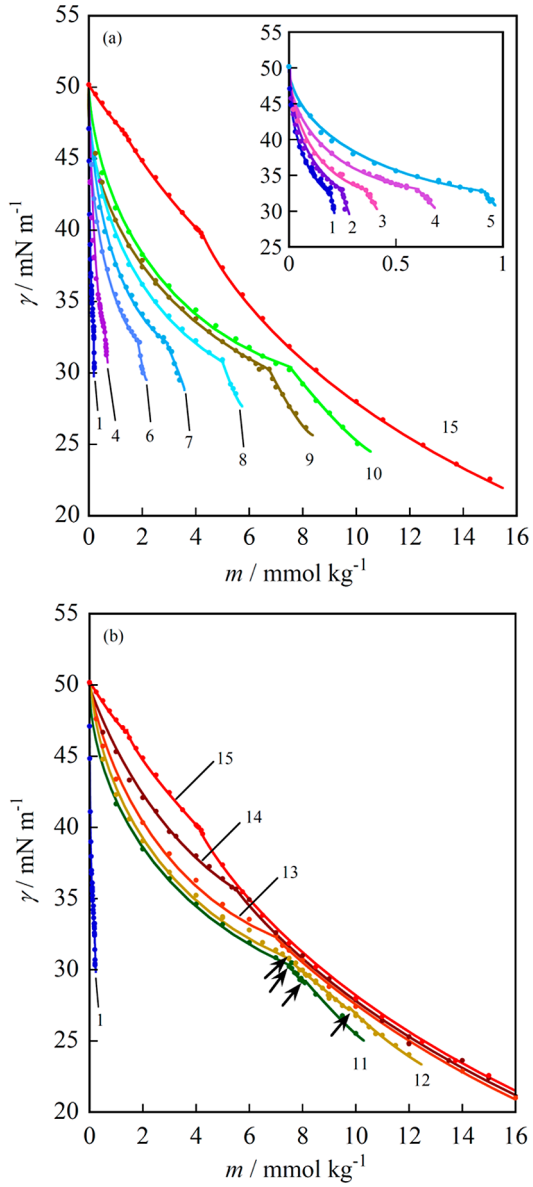

Figure 1. (a) Interfacial tension vs total molality curves at constant bulk composition: X_2 = (1) 0 (FC_{10}diol), (2) 0.25, (3) 0.5, (4) 0.7, (5) 0.8, (6) 0.9, (7) 0.94, (8) 0.965, (9) 0.975, (10) 0.98, (15) 1 ($FC_{10}OH$). The size of the circle is equivalent to the error bar of interfacial tension. (b) Interfacial tension vs total molality curves at constant bulk composition: X_2 = (1) 0 (FC_{10}diol), (11) 0.982, (12) 0.985, (13) 0.99, (14) 0.995, (15) 1 ($FC_{10}OH$). The size of the circle is equivalent to the error bar of interfacial tension.

Here, y_1^O and y_2^O are respectively the partial molar entropy ($y = s$) and volume ($y = v$) of FC_{10}diol and $FC_{10}OH$ in the hexane solution.

The total interfacial density Γ^H was calculated by applying the equation

$$\Gamma^H = -(m/RT)(\partial\gamma/\partial m)_{T,p,X_2} \quad (17)$$

to the γ vs m curves in Figure 1. The results are shown as the Γ^H vs m curves below and above X_2 = 0.9 in Figure 4a,b, respectively. The Γ^H values increase with increasing m and change discontinuously at the phase transition points. Below X_2 = 0.98 (curves 1–10), the value once converges into around 2–3 μmol m^{-2}, just below the phase transition and then increases discontinuously to 7–9 μmol m^{-2}, which is much larger than that of condensed $FC_{10}OH$ monolayer, in which the molecules orient normally to the interface. The Γ^H value above the phase transition in $X_2 \geq 0.99$ (curves 13 and 14), on the other hand, is around 5.7 μmol m^{-2} almost equal to the Γ^H value in the condensed $FC_{10}OH$ monolayer. It is noted that the Γ^H values at X_2 = 0.982 (curve 11) and 0.985 (curve 12) change

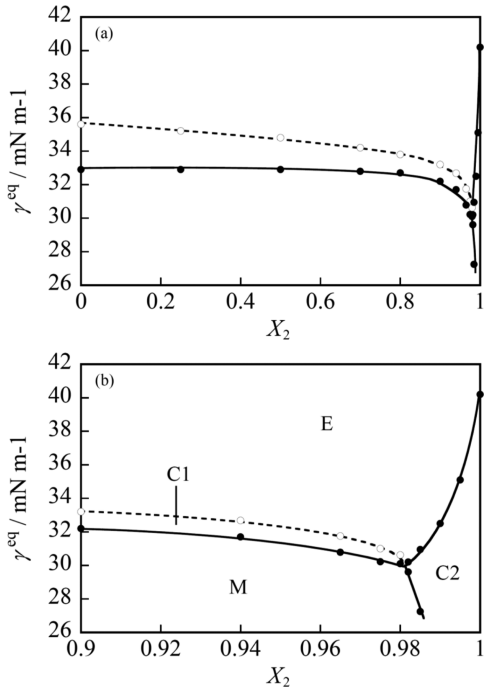

Figure 2. Interfacial tension vs bulk composition curves at phase transition points (solid lines) and the boundary between E and C1 states (dashed line): (a) in a whole X_2 region; (b) in $X_2 \geq 0.9$ region.

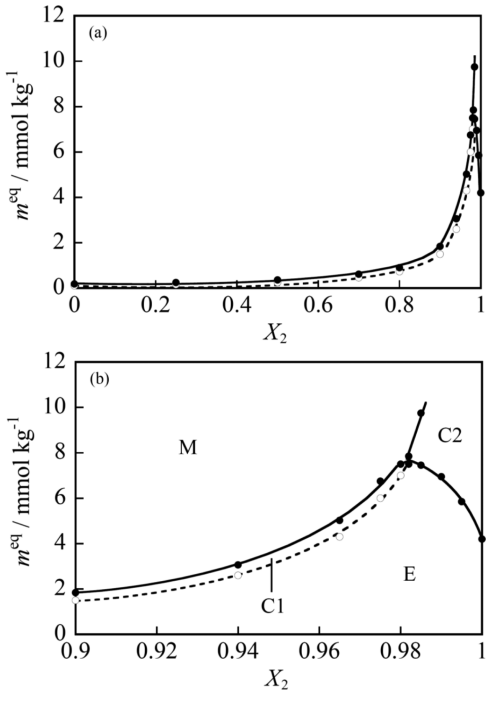

Figure 3. Total molality vs bulk composition curves at phase transition points (solid lines) and the boundary between E and C1 states (dashed line): (a) in a whole X_2 region; (b) in $X_2 \geq 0.9$ region.

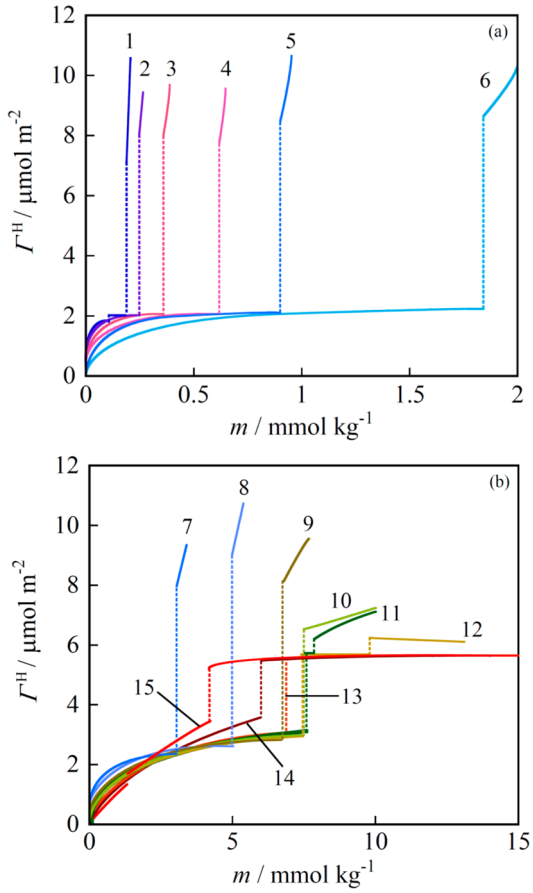

Figure 4. (a) Total interfacial density vs total molality curves at constant bulk composition in the $X_2 \leq 0.9$ region: X_2 = (1) 0 (FC_{10}diol), (2) 0.25, (3) 0.5, (4) 0.7, (5) 0.8, (6) 0.9. (b) Total interfacial density vs total molality curves at constant bulk composition in the $X_2 > 0.9$ region: X_2 = (7) 0.94, (8) 0.965, (9) 0.975, (10) 0.98, (11) 0.982, (12) 0.985, (13) 0.99, (14) 0.995, (15) 1 (FC_{10}OH).

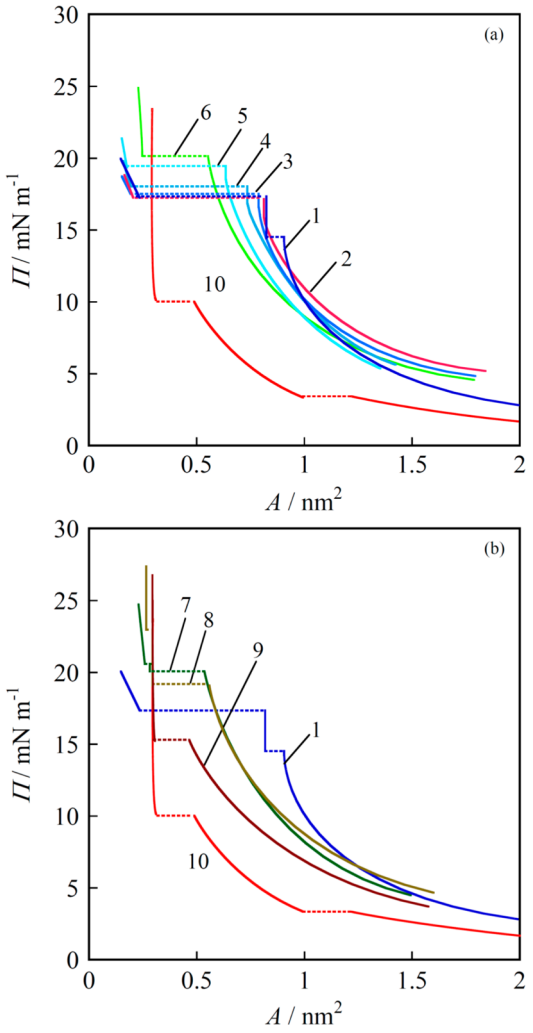

Figure 5. (a) Interfacial pressure vs mean molecular area curves at constant bulk composition: X_2 = (1) 0 (FC_{10}diol), (2) 0.5, (3) 0.8, (4) 0.9, (5) 0.965, (6) 0.98, (10) 1 (FC_{10}OH). (b) Interfacial pressure vs mean molecular area curves at constant bulk composition: X_2 = (1) 0 (FC_{10}diol), (7) 0.982, (8) 0.985, (9) 0.995, (10) 1 (FC_{10}OH).

discontinuously from 3.0 μmol m^{-2} just below to 5.7 μmol m^{-2} above the first phase transition, and then jump to 6 μmol m^{-2} above the second transition.

To clarify the state of adsorbed film, the Π vs A curves are drawn in Figure 5. Here, the Π and A values were calculated by the equations

$$\Pi = \gamma^0 - \gamma \tag{18}$$

and

$$A = 1/N_A\Gamma^H \tag{19}$$

where γ^0 is the interfacial tension at the pure hexane/water interface and N_A is Avogadro's number. The Π vs A curves below X_2 = 0.98 (curve 2−6) consist of two parts connected by a discontinuous change at the phase transition point. Below the transition pressure, the A values decrease gradually with increasing Π, and the curves just below the transition become almost vertical, indicating that the adsorbed film takes a condensed state (state C1) in this region. It is noticeable that the A values in the C1 state decrease gradually from the value of pure FC_{10}diol system (0.82 nm^2) with increasing X_2. Above the transition point, on the other hand, the A values are much smaller than the cross-sectional area of FC chain, and therefore the formation of a multilayer (state M) is highly suggested.

In $X_2 \geq 0.99$, the Π vs A curves also consist of two parts (curve 9 in Figure 5a,b). The A value below the transition pressure decreases continuously with increasing Π, and that above the transition is almost constant at 0.29 nm^2 against the increase in Π, suggesting that all molecules orient normally to the interface. Taking note of that the shape of the curve is very similar to that of pure FC_{10}OH system, it is reasonable that the phase transition between the expanded (state E) and condensed (state C2) states takes place in the adsorbed films above X_2 = 0.99.

At X_2 = 0.982 (curve 7) and 0.985 (curve 8), furthermore, two kinds of phase transitions, i.e., the E−C2 transition at low and the C2−M transition at high Π, take place in the adsorbed film. According to the classification of the Π vs A curves, therefore, we can assign the film state as shown in Figures 2 and 3. The dashed lines in Figures 2 and 3, respectively, show the γ and m values below and above which the Π vs A curve becomes vertical; i.e., they are the boundaries between the expanded (E) and condensed monolayer (C1).

To elucidate the miscibility of FC_{10}diol and FC_{10}OH molecules in the adsorbed film, first, the film composition of FC_{10}OH was calculated by applying the equation[34]

$$X_2^H = X_2 - (X_1X_2/m)(\partial m/\partial X_2)_{T,p,\gamma} \quad (20)$$

to the m vs X_2 curves at given T, p, and γ. In Figure 6a are shown the m vs X_2^H curves together with the m vs X_2 curves at

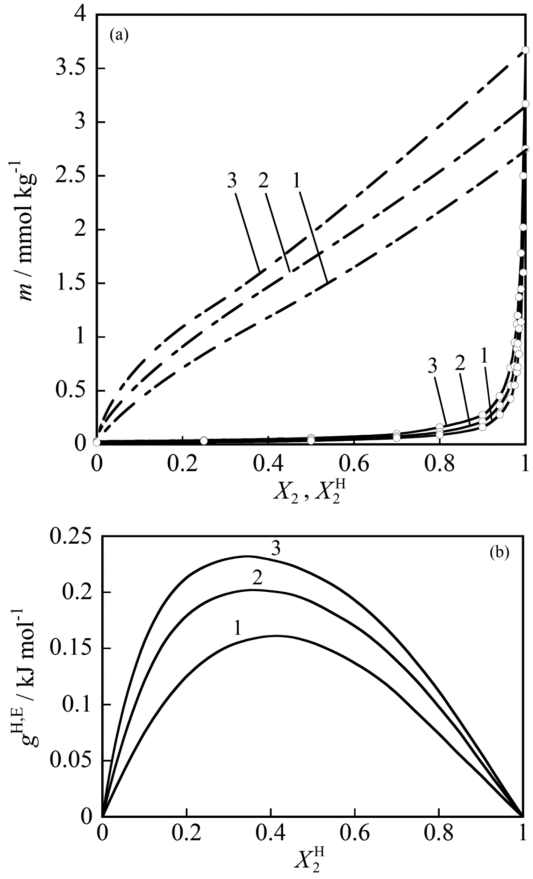

Figure 6. (a) Phase diagrams of adsorption at constant interfacial tension: (−) m vs X_2 curve, (−·−) m vs X_2^H curve; γ = (1) 43 mN m^{-1}; (2) 42 mN m^{-1}; (3) 41 mN m^{-1}. (b) Excess Gibbs energy of adsorption vs film composition curves at constant interfacial tension: γ = (1) 43 mN m^{-1}; (2) 42 mN m^{-1}; (3) 41 mN m^{-1}.

the given γ. These are the phase diagrams of adsorption (PDA), which provide a quantitative relation of compositions between adsorbed film and bulk solution. The PDAs at γ = 43, 42, and 41 mN m^{-1} are the ones of the E state at whole X_2. It is seen that the m vs X_2^H curves are located above the line of the criterion of ideal mixing of molecules in the adsorbed film that is the straight line connecting the molalities, m_1^0 and m_2^0, of individual components at a given γ as[34]

$$m = m_1^0 + (m_2^0 - m_1^0)X_2^H \quad (21)$$

The positive deviation of the m vs X_2^H curve from the criterion indicates that the mixing of FC_{10}diol and FC_{10}OH in the E state is unfavorable compared to the ideal mixing. This is mainly due to the loss of dispersion interaction by mixing of parallel-oriented FC_{10}diol with normal-oriented FC_{10}OH in the adsorbed film.

The nonideal mixing of molecules is further examined by the excess Gibbs energy of adsorption $g^{H,E}$ calculated by the following equation[34]

$$g^{H,E} = RT(X_1^H \ln f_1^H + X_2^H \ln f_2^H) \quad (22)$$

where f_i^H (i = 1, 2) is the activity coefficient of component i in the adsorbed film defined symmetrically as $f_i^H \to 1$, when $X_i^H \to 1$, and calculated by

$$f_i^H = X_i m / X_i^H m_i^0 \quad (23)$$

The results are shown as the $g^{H,E}$ vs X_2^H curves at constant γ in Figure 6b. The $g^{H,E}$ value is positive and increases with decreasing γ. Thus, the excess area in the adsorbed film $A^{H,E}$ estimated by[8,34]

$$A^{H,E} = -(1/N_A)(\partial g^{H,E}/\partial\gamma)_{T,p,X_2^H} \quad (24)$$

at γ = 42 mN m^{-1} is positive in a whole X_2^H region. The mixing of FC_{10}diol and FC_{10}OH in the adsorbed film is accompanied by an increase in an occupied area because the mutual interaction is weaker between the different molecules than between the same ones. The maximum value is 0.06 nm^2 at most, however, which is much smaller than the positive $A^{H,E}$ (~0.3 nm^2) obtained in the expanded state of 1-icosanol (C_{20}OH)−FC_{10}OH mixture.[8]

Figure 7 shows the m vs X_2 curves (solid lines) at γ = 31.7 (curve 1) and 27.3 mN m^{-1} (curve 2); the curves above $X_2 \geq$

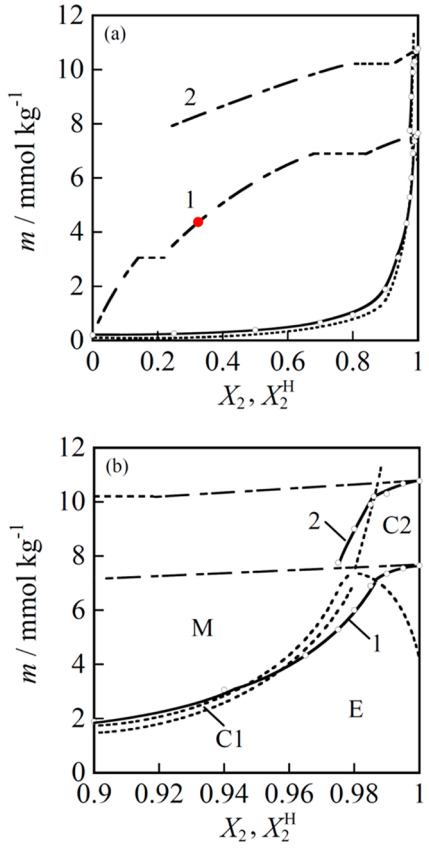

Figure 7. Phase diagrams of adsorption at constant interfacial tension: (−) m vs X_2 curve; (−·−) m vs X_2^H curve; (− − −) m^{eq} vs X_2^H curve; γ = (1) 31.7 mN m^{-1}; (2) 27.3 mN m^{-1}.

0.9 are magnified in Figure 7b. At γ = 31.7 mN m^{-1}, the curve intersects with the m^{eq} vs X_2 curves, which are shown by dashed lines, at three points (X_2 = 0.94, 0.957, and 0.988). The adsorbed film takes the M state below X_2 = 0.94, C1 state in 0.94 ≤ X_2 ≤ 0.957, the E state in 0.957 < X_2 ≤ 0.988, and the C2 state above X_2 = 0.988. The m vs X_2 curve at γ = 27.3 mN m^{-1} intersects the curve of the M (X_2 ≤ 0.985)−C2 (0.985 ≤

$X_2 \leq 1$) phase transition point. The m vs X_2^H curves (chain dotted lines) at these γ values are shown together with the m vs X_2 curves in Figure 7. It is seen that the X_2^H value changes discontinuously accompanied by the phase transition, whereas continuously between E and C1 states (the boundary point between E and C1 is denoted as red circle), and the m vs X_2^H curves slightly convex upward, suggesting the positive deviation from the ideal mixing.

The composition diagram, m^{eq} vs X_2^H curves at the phase transition points are drawn in Figure 8. Here, the horizontal

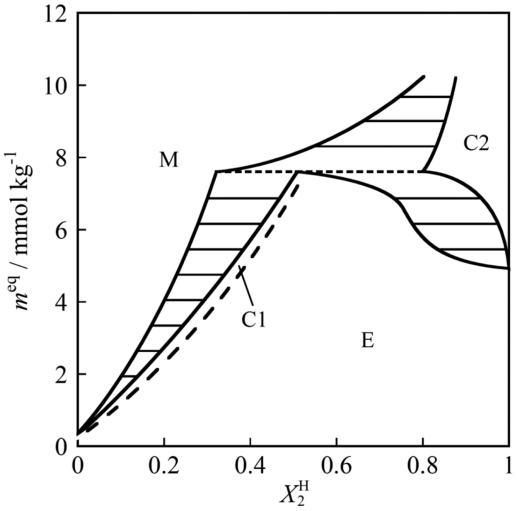

Figure 8. Total molality vs film composition curves at phase transition points (solid lines) and the boundary between E and C1 states (broken lines).

lines connecting the film compositions between two film states in equilibrium at the transition point are the tie lines, except for the E−C1 transition at which the X_2^H value changes continuously (the boundary is described by dashed line). The diagram is a eutectic type, which reflects the low miscibility of FC_{10}diol and FC_{10}OH. In particular, the C2 state appears in a limited composition region close to pure FC_{10}OH. Furthermore, the noticeable point is that the M state is richer in FC_{10}diol than in FC_{10}OH when the molecules pile on the C1 state, whereas the M state evolved from the C2 state can be richer in FC_{10}OH than in FC_{10}diol; the miscibility of molecules in the M state varies depending on the structure of the condensed monolayer. The structures of condensed monolayers (C1 and C2 states) as well as the M state will be clarified in the latter part of this paper.

The mean molecular area A are plotted against the film composition X_2^H in Figure 9. At γ = 42 mN m^{-1} (E state), the A vs X_2^H plots deviate positively from the straight line, $A = X_1^H A_1^0 + X_2^H A_2^0$, for an ideal mixing of molecules in the adsorbed film but agree well with the solid one given by

$$A = A^{H,E} + X_1^H A_1^0 + X_2^H A_2^0 \quad (25)$$

where A_i^0 is the mean molecular area of component i in the pure system and $A^{H,E}$, the value calculated by eq 24, was used for drawing the solid line, manifesting the nonideal mixing of FC_{10}diol and FC_{10}OH in the E state.

In the C2 state at γ = 31.2 mN m^{-1} (gray squares), the A value is independent of X_2^H and almost equals that of the FC_{10}OH pure system, suggesting that all molecules orient normally to the interface in harmony with the Π vs A curve in

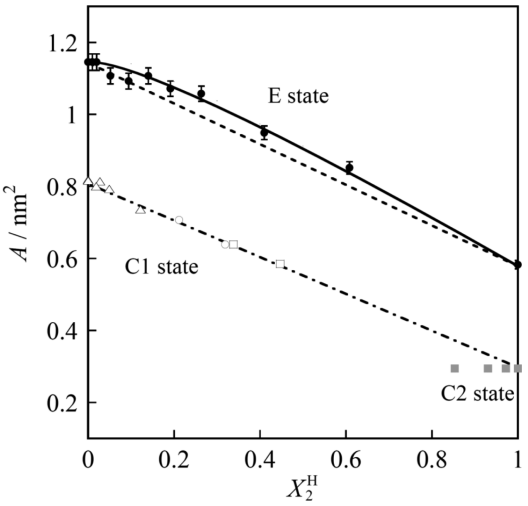

Figure 9. Mean molecular area vs film composition plots at given interfacial tension: solid square, γ = 42 mN m^{-1}; white triangle, 33 mN m^{-1}; white circle, 31.7 mN m^{-1}; white square, 31 mN m^{-1}; gray square, 31.2 mN m^{-1}; (−): eq 25, (−·−): eq 26

the C2 state, as shown above. On the other hand, the A values in the C1 state (white plots) decrease linearly with increasing X_2^H and are almost satisfied with the linear relation given by

$$A = X_1^H A_1^{0,C} + X_2^H A_2^{0,C} \quad (26)$$

where $A_i^{0,C}$ is the mean molecular area of solute i in the condensed states of pure systems: $A_1^{0,C}$ = 0.82 nm^2 and $A_2^{0,C}$ = 0.29 nm^2. Because it was demonstrated that the mixing of FC_{10}diol and FC_{10}OH in the adsorbed film is not favorable, the agreement of both plots and line strongly suggests the microscopic phase separation in the adsorbed film; parallel-oriented FC_{10}diol and normal-oriented FC_{10}OH condensed domains coexist in the C1 state. In this situation, the X_2^H value in eq 26 corresponds to the coverage of FC_{10}OH domain. These expectations will be further examined by X-ray reflectivity measurements.

The piling of molecules was further examined by evaluating the change in interfacial densities of individual components associated with the phase transition from condensed monolayer to multilayer $\Delta\Gamma_i^H$ defined by

$$\Delta\Gamma_i^H = \Delta\Gamma_i^{H,M} - \Delta\Gamma_i^{H,CX} \quad (i = 1 \text{ or } 2) \quad (27)$$

where M and CX (X = 1 or 2) indicate respectively the multilayer and condensed monolayer states. The results are shown as the $\Delta\Gamma_i^H$ vs X_2 curves in Figure 10; the curves in $X_2 \geq$ 0.9 are magnified in Figure 10b. The $\Delta\Gamma_1^H$ value is positive for both C1−M ($X_2 \leq 0.981$) and C2−M ($X_2 > 0.981$) transitions, and therefore FC_{10}diol molecules pile spontaneously on C1 and C2 monolayers. On the other hand, the $\Delta\Gamma_2^H$ value is small positive for the C1−M transition, and negative for the C2−M one, indicating that small amounts of FC_{10}OH molecules pile with FC_{10}diol on the C1 monolayer but are expelled accompanied by piling of FC_{10}diol molecules on the C2 monolayer. At the C1−M transition, the $\Delta\Gamma_1^H$ value is much larger than $\Delta\Gamma_2^H$, and thus FC_{10}diol is more dominant in the multilayer formation than FC_{10}OH. Taking note of our previous finding that FC_{10}diol piles spontaneously with parallel orientation in the multilayer of its single component system, it is suggested that the FC_{10}diol molecules in the M state evolved from the C1 monolayer are lying parallel to the interface. In the

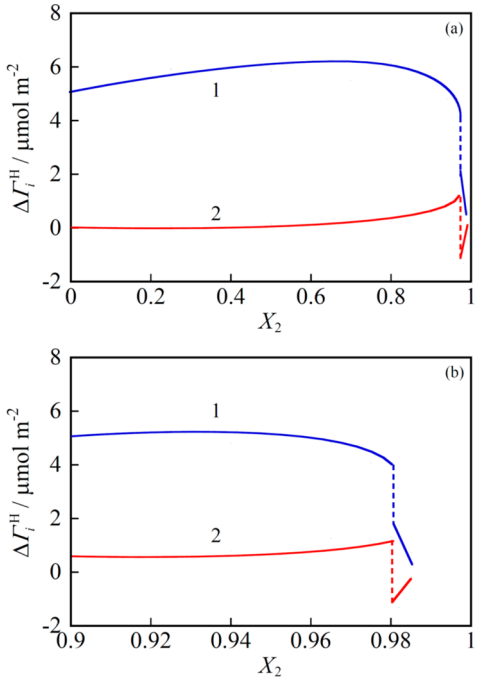

Figure 10. Changes in interfacial density of individual components associated with the phase transition from condensed monolayer to multilayer states: (a) in a whole X_2 region; (b) in $X_2 \geq 0.9$ region; (1) FC_{10}diol; (2) FC_{10}OH.

case of the C2−M transition, the space for adsorption of FC_{10}diol with parallel orientation may be produced by the desorption of normal-oriented FC_{10}OH, and then further piling of FC_{10}diol is promoted to form a multilayer.

X-ray Reflectivity. To clarify the structure of the adsorbed film, the X-ray reflection was applied to the adsorbed films of the present mixture as well as those of pure components. The X-ray reflectivity normalized by Fresnel reflectivity R/R_F obtained for the condensed and multilayer states of the pure FC_{10}diol at m_1 = 0.16 and 0.198 mmol kg^{-1}, respectively, and for the condensed state of FC_{10}OH at m_2 = 8.0 mmol kg^{-1} are plotted against the scattering vector Q_z in Figure 11a. Attempts were made to fit these plots by using the one-slab model in which the adsorbed film is assumed to have a structure consisting of one slab with uniform electron density and thickness. In this model, the slab thickness L_1 and the electron density of the slab normalized by that of pure water ρ_1/ρ_w were used as the fitting parameters, where the roughness σ was fixed to the one of capillary wave contribution. The results are shown by black lines; the curves fit the plots very well. In Figure 11b are shown the electron density profiles, and the L_1 and ρ_1/ρ_w values are summarized in Table 1. The L_1 value of FC_{10}OH is 9.9 Å, which is nearly equal to the calculated length of FC chain of the molecule and the corresponding electron density (ρ_1/ρ_w = 1.8) is very close to that of solid fluoroalkane (ρ_1/ρ_w = 1.9). Therefore, it is concluded that the FC_{10}OH molecules are densely packed with normal molecular orientation in the condensed monolayer state.

In the case of the FC_{10}diol system, on the other hand, the L_1 value (5.7 Å) in the condensed state is much smaller than that in the condensed FC_{10}OH monolayer but is almost equal to the diameter of the cross section of FC chain (5.9 Å), manifesting that FC_{10}diol molecules are lying almost parallel to the interface. Furthermore, the ρ_1/ρ_w value of 1.4 is also close to

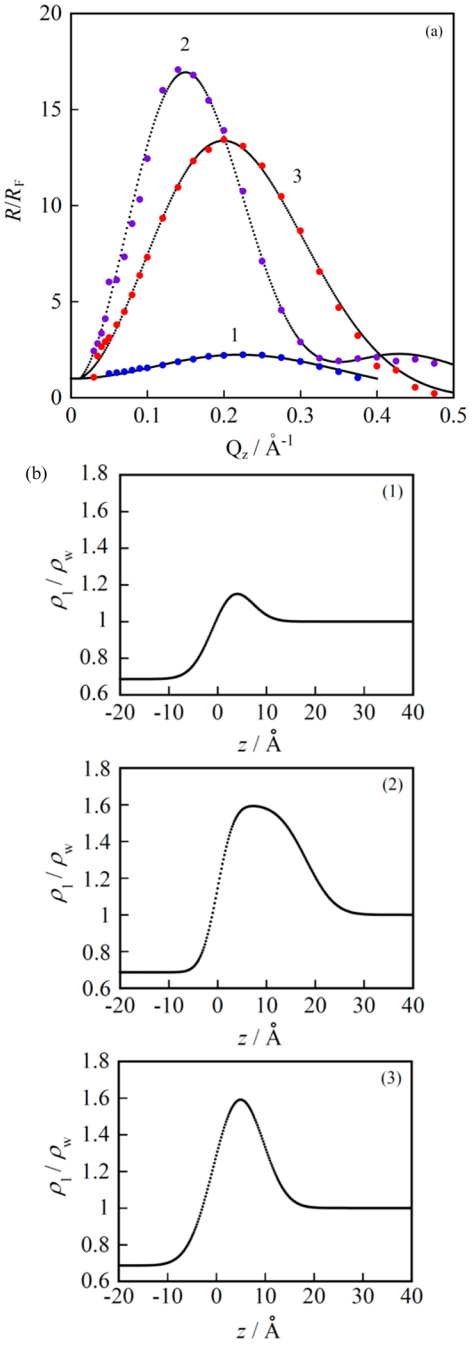

Figure 11. (a) X-ray reflectivity normalized by Fresnel reflectivity vs scattering vector plots. The dotted lines are fitted curves by the one-slab model: (1) condensed monolayer of FC_{10}diol at m_1 = 0.16 mmol kg^{-1}; (2) multilayer of FC_{10}diol at m_1 = 0.198 mmol kg^{-1}; (3) condensed monolayer of FC_{10}OH at m_2 = 8.0 mmol kg^{-1}. (b) Electron density profiles along the interface normal: (1) condensed monolayer of FC_{10}diol at m_1 = 0.16 mmol kg^{-1}; (2) multilayer of FC_{10}diol at m_1 = 0.198 mmol kg^{-1}; (3) condensed monolayer of FC_{10}OH at m_2 = 8.0 mmol kg^{-1}.

the value estimated for the case that the FC_{10}diol molecules are densely packed with parallel orientation (ρ_1/ρ_w = 1.4−1.6). For the FC_{10}diol multilayer state, the L_1 value is 18.1 Å, which is much larger than that obtained for the condensed FC_{10}OH film, and therefore FC_{10}diol molecules pile spontaneously and successively to form a multilayer. Taking note of the parallel orientation of FC_{10}diol in the condensed monolayer, it is

Table 1. Fitting Parameters Obtained by One-Slab Model Fitting of X-ray Reflectivity Measurement in Pure Component Systems

	m/mmol kg^{-1}	state	L_1/Å	ρ_1/ρ_w	σ/Å
FC_{10}diol	0.16	condensed	5.7	1.4	3.7
FC_{10}diol	0.198	multilayer	18.1	1.6	3.7
FC_{10}OH	8.0	condensed	9.9	1.8	4.0

reasonable that the molecules pile with parallel orientation in the multilayer as well; the L_1 value suggests around three layers in the multilayer. Furthermore, the electron density in the multilayer, ρ_1/ρ_w, is 1.6, indicating slightly denser molecular packing in the multilayer than in the monolayer, probably due to the effective dispersion interaction between hydrophobic chain and hydrogen bonding between piling molecules in the multilayer.

For the condensed monolayer of the mixed system, the R/R_F vs Q_z plots measured in the C1 and C2 states are shown in Figure 12a. It is clearly seen that the intensity is much lower in

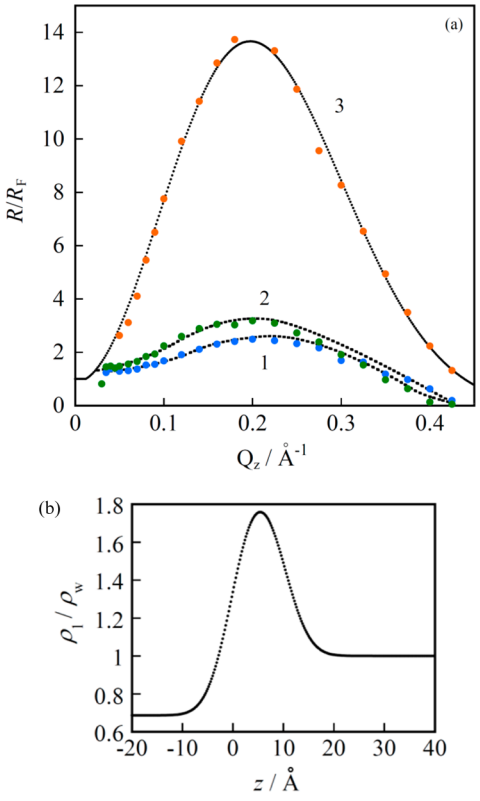

Figure 12. (a) X-ray reflectivity normalized by Fresnel reflectivity vs scattering vector plots: (1) C1 state at m_1 = 1.7 mmol kg^{-1} and X_2 = 0.9; (2) C1 state at m_1 = 6.0 mmol kg^{-1} and X_2 = 0.975; (3) C2 state at m_2 = 8.5 mmol kg^{-1} and X_2 = 0.985. The dotted lines are fitted curves by the domain model (plots (1) and (2)) and the one-slab model (plot (3)). (b) Electron density profiles along the interface normal: C2 state at m = 8.5 mmol kg^{-1} and X_2 = 0.985.

the C1 state (plots 1 and 2) than in the C2 one (plot 3). The R/R_F vs Q_z plot measured at X_2 = 0.985 is almost the same as that of the condensed monolayer of the FC_{10}OH pure system (curve 3 in Figure 11a). Thus, the plot was well fitted by one-slab model with almost the same electron density profile as shown in Figure 12b; L_1 and ρ_1/ρ_w values are listed in Table 2. Taking note of the finding from PDA in Figure 7b that FC_{10}diol and FC_{10}OH molecules are miscible in the C2 state, this result clearly indicates that both molecules orient perpendicularly to the interface and are closely packed with each other.

Table 2. Fitting Parameters Obtained by One-Slab Model Fitting of X-ray Reflectivity Measurement in Mixed Systems

X_2	m/mmol kg^{-1}	state	L_1/Å	ρ_1/ρ_w	σ/Å
0.985	8.5	C2	10.4	1.8	3.9
0.975	7.0	M	16.7	1.4	3.9
0.985	10.5	M	13.2	1.6	3.8

The shapes of R/R_F vs Q_z plots in the C1 state at X_2 = 0.9 and 0.975 are similar to that of the pure FC_{10}diol system (curve 1 in Figure 11a). In these cases, we tried to fit the plots by using the "domain model" in which the adsorbed film is assumed to consist of two coexisting kinds of domains and the intensity is given by eq 10 for coherent and eq 11 for incoherent interference. The values of $R_1(Q_z)$ and $R_2(Q_z)$ (or r_1 and r_2) were chosen to be the reflectivities (or amplitudes) determined from the fitting to the condensed monolayers of pure systems. The area coverage of FC_{10}OH domain, which is the fraction of the interface covered by the domain, C_X, is a fitting parameter. Although both the coherent and incoherent models give good fitting, we concluded that the fitting by using coherent model is better than that by the incoherent one because the C_X values agree well with those estimated from the thermodynamic analysis, C_T

$$1/A = (1 - C_T)/A_1^{0,C} + C_T/A_2^{0,C} \quad (28)$$

The estimated C_X and C_T values are listed in Table 3. This result confirms that the C1 state is heterogeneous, consisting of

Table 3. Domain Area Coverages Obtained by Domain Model Fitting of X-ray Reflectivity Measurement and by Interfacial Tension Measurement in Mixed Systems

X_2	m/mmol kg^{-1}	state	C_X	C_T
0.9	1.7	C1	0.16	0.22
0.975	6.0	C1	0.05	0.06

two kinds of domains: parallel-oriented FC_{10}diol and normal-oriented FC_{10}OH domains with the size smaller than the coherent length of the X-ray of about 5 μm.

The coexistence of parallel-oriented and normal-oriented domains was also observed in the condensed monolayer of the FC_{10}diol and 1*H*,1*H*,2*H*,2*H*-perfluorododecanol (FC_{12}OH) mixture at the hexane/water interface.[35] In the C1 state, however, the film composition of FC_{12}OH, X_2^H, i.e., the coverage of the FC_{12}OH domain, converges to 0.14 against the increase in X_2, which is in striking contrast to our finding that the coverage of the FC_{10}OH domain increases up to about 0.5 with increasing X_2 in the present system. Because it is reasonable that the dispersion interaction between a parallel-oriented FC_{10}diol molecule and normal-oriented FC_nOH one does not have a significant effect on their miscibility in the C1 state, one of the crucial factors to determine the domain coverage will be line tension τ, which is the excess free energy accompanied by the formation of a boundary line between coexisting domains. The τ value is roughly estimated by[36]

$$\tau = \gamma^{DS}\Delta L \quad (29)$$

where γ^{DS} is the interfacial tension between the material forming thicker domain (i.e., FC_nOH) and surrounding

dx.doi.org/10.1021/jp507049z | J. Phys. Chem. B 2014, 118, 12451−12461

medium and ΔL is the thickness gap between the two domains. In the C1 state, we employed $\gamma^{DS} \approx 1.5$ mN m^{-1} as the interfacial tension between perfluoroalkane and hexane because the hydrophobic chain of FC_nOH on the boundary of the normal-oriented domain is assumed to contact preferentially with hexane. The ΔL value is 1.0 nm for the FC_{10}diol–$FC_{10}OH$ system and 1.3 nm for the FC_{10}diol–$FC_{12}OH$ one. The τ value is smaller in the former than in the latter. This may promote the formation of a larger $FC_{10}OH$ domain compared to the $FC_{12}OH$ one.

The R/R_F vs Q_z plots measured in the M state at $X_2 = 0$, 0.975, and 0.985 are shown in Figure 13a. The black lines are

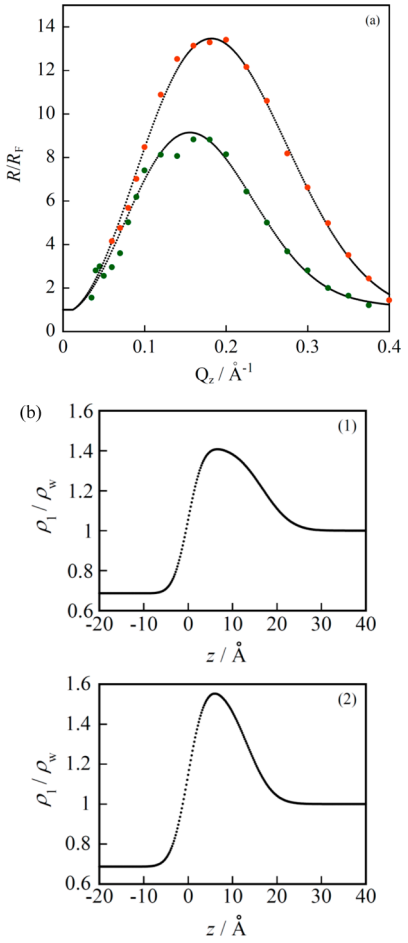

Figure 13. (a) X-ray reflectivity normalized by Fresnel reflectivity vs scattering vector plots: The dotted lines are fitted curves by the one-slab model: (1) multilayer state at $m = 7.0$ mmol kg^{-1} and $X_2 = 0.975$; (2) multilayer state at $m = 10.5$ mmol kg^{-1} and $X_2 = 0.985$. (b) Electron density profiles along the interface normal: (1) multilayer state at $m = 7.0$ mmol kg^{-1} and $X_2 = 0.975$, (2) multilayer state at $m = 10.5$ mmol kg^{-1} and $X_2 = 0.985$.

the fitted ones by using one-slab model. It is realized that both curves trace the plot very well. The electron density profiles determined and the fitting parameters are shown in Figure 13b and Table 2, respectively. The layer thickness is larger in the M state than in the C2 state (~10 Å), which clearly indicates the piling of molecules. Furthermore, the thickness value at $X_2 = 0.985$ is smaller than those at $X_2 = 0$ and 0.975. This result is consistent with the small increase in the interfacial density accompanied by the formation of a multilayer at $X_2 = 0.985$.

CONCLUSIONS

The effect of molecular orientation on the miscibility of molecules and structure of the adsorbed film of FC_{10}diol and $FC_{10}OH$ mixture at the hexane/water interface were examined by interfacial tension and X-ray reflectivity measurements. Two kinds of condensed monolayers (C1 and C2) and multilayer (M) states appeared depending on the total molality m and the composition of $FC_{10}OH$ in the mixture X_2. Combining the results of PDA and the electron density profile in the C2 state, it was concluded that $FC_{10}OH$ and FC_{10}diol molecules are miscible and densely packed with the molecular orientation perpendicular to the interface. The C1 state, on the other hand, is a heterogeneous structure in which the normal- and parallel-oriented domains coexist at the interface. The interfacial coverage of the normal-oriented domain agrees well with that calculated from the film composition by thermodynamic data analysis and was reasonably explained by domain line tension estimated by the interfacial tension between the material forming a thicker domain and surrounding medium and the thickness gap between the two domains; the lower domain line tension promotes the formation of larger amount of normal-oriented domain. The measurement of line tension by BAM (Brewster angle microscopy) observation of domains is further necessary to discuss precisely the effect of line tension on the formation of heterogeneous structure in the adsorbed film.

AUTHOR INFORMATION

Corresponding Author

*T. Takiue. Phone: +81 92 642 2578. Fax: +81 92 642 2607. E-mail: t.takiue@chem.kyushu-univ.jp.

Notes

The authors declare no competing financial interest.

ACKNOWLEDGMENTS

This work was supported in part by the *Grant-in-Aid for Scientific Research on Innovative Areas* (Soft Interface Science) of the Ministry of Education, Culture, Sports, Science and Technology of Japan (No. 23106715). The X-ray reflectivity measurements were performed at BL37XU in SPring-8 under the approval of Japan Synchrotron Research Institute (Nos. 2012A1203, 2012B1154 and 2013A1339).

REFERENCES

(1) McConnell, H. M.; Vrljic, M. Liquid-liquid immiscibility in membranes. *Annu. Rev. Biophys. Biophys. Struct.* **2003**, *32*, 469–492.

(2) Fanani, M. L.; Maggio, B. J. Liquid-liquid domain miscibility driven by composition and domain thickness in ternary lipid monolayers. *J. Phys. Chem. B* **2001**, *115*, 41–49.

(3) Stottrup, B. L.; Stevens, D. S.; Keller, S. L. Miscibility of ternary mixtures of phospholipids and cholesterol in monolayers, and application to bilayer systems. *Biophys. J.* **2005**, *88*, 269–276.

(4) Takiue, T.; Vollhardt, D. Miscibility of alkanol and fluoroalkanol in Langmuir film at the air/water interface. *Colloids Surf.m A* **2002**, *198–200*, 797–804.

(5) Krafft, M. P.; Goldmann, M. Monolayers made from fluorinated amphiphiles. *Curr. Opin. Colloid Interface Sci.* **2003**, *8*, 243–250.

(6) Bernardini, C.; Stoyanov, S. D.; Arnaudov, L. N.; CohenStuart, M. A. Colloids in flatland: a perspective on 2D phase-separated systems, characterization methods and lineactant design. *Chem. Soc. Rev.* **2013**, *42*, 2100–2129.

(7) Takiue, T.; Matsuo, T.; Ikeda, N.; Motomura, K.; Aratono, M. Thermodynamic study on phase transition in adsorbed film of fluoroalkanol at the hexane/water interface. 4. Phase transition in the

adsorbed film of the alkanol and fluoroalkanol mixture. *J. Phys. Chem. B* **1998**, *102*, 4906−4911.
(8) Takiue, T.; Matsuo, T.; Ikeda, N.; Motomura, K.; Aratono, M. Thermodynamic study on phase transition in adsorbed films of fluoroallanol at the hexane/water interface. 5. Miscibility in the adsorbed film of an alkanol and fluoroalkanol mixture. *J. Phys. Chem. B* **1998**, *102*, 5840−5844.
(9) Pingali, S. L.; Takiue, T.; Luo, G.; Tikhonov, A. M.; Ikeda, N.; Aratono, M.; Schlossman, M. L. X-ray studies of surfactant ordering and interfacial phases at the water-oil interface. *J. Dispersion Sci. Technol.* **2006**, *27*, 715−722.
(10) Pingali, S. L.; Takiue, T.; Luo, G.; Tikhonov, A. M.; Ikeda, N.; Aratono, M.; Schlossman, M. L. X-ray reflectivity and interfacial tension study of the structure and phase behavior of the interface between water and mixed surfactant solutions of $CH_3(CH_2)_{19}OH$ and $CF_3(CF_2)_7(CH_2)_2OH$ in Hexane. *J. Phys. Chem. B* **2005**, *109*, 1210−1225.
(11) Veatch, S. L.; Keller, S. L. Seeing spots: Complex phase behavior in simple membranes. *Biochem. Biophys. Acta* **2005**, *1746*, 172−185.
(12) Veatch, S. L.; Gowrisch, K.; Keller, S. L. Closed-loop miscibility gap and quantitative tie-lines in ternary membranes containing diphytanoyl PC. *Biophys. J.* **2006**, *90*, 4428−4436.
(13) Almeida, R. F. M.; Fedorov, A.; Priet, M. Sphingomyelin/ phosphatidylcholine/ cholesterol phase diagram: Boundaries and composition of lipid rafts. *Biophys. J.* **2003**, *85*, 2406−2419.
(14) Rietveld, A.; Simons, K. The differential miscibility of lipids as the basis for the formation of functional membrane rafts. *Biochem. Biophys. Acta* **1998**, *1376*, 467−479.
(15) Lingwood, D.; Simons, K. Lipid rafts as a membrane-organizing principle. *Science* **2010**, *327*, 46−50.
(16) London, E. How principles of domain formation in model membranes may explain ambiguities concerning lipid raft formation in cells. *Biochem. Biophys. Acta* **2005**, *1746*, 203−230.
(17) Takiue, T.; Hirose, D.; Murakami, D.; Sakamoto, H.; Matsubara, H.; Aratono, M. Effect of ω-hydrogenation on the adsorption of fluorononanols at the hexane/water interface: Pressure effect on the adsorption of fluorononanols. *J. Phys. Chem. B* **2005**, *109*, 16429−16434.
(18) Takiue, T.; Murakami, D.; Tamura, T.; Sakamoto, H.; Matsubara, H.; Aratono, M. Effect of ω-hydrogenation on the adsorption of fluorononanols at the hexane/water interface: Temperature effect on the adsorption of fluorononanols. *J. Phys. Chem. B* **2005**, *109*, 14154−14159.
(19) Murakami, D.; Takata, Y.; Matsubara, H.; Aratono, M.; Takiue, T. Effect of ω-hydrogenation on the adsorption of fluorononanols at the hexane/water interface: Miscibility in the adorbed film of fluorononanols. *J. Phys. Chem. B* **2005**, *109*, 22366−22370.
(20) Pal, R. P.; Chatterjee, A. K.; Chattoraj, D. K. Adsorption of the organic dibasic acids at the liquid interfaces. *J. Colloid Interface Sci.* **1975**, *52*, 46−55.
(21) Ikeda, K.; Yasuda, M.; Ishikawa, M.; Esumi, K.; Meguro, K.; Binana-Limbele, W.; Zana, R. Physicichemical properties of α,ω-type bolaform surfactant in aqueous solution. Eicosane-1,20-bis-(triethylammonium bromide). *Colloid Polym. Sci.* **1989**, *267*, 825−30.
(22) Menger, F. M.; Wrenn, S. Interfacial and miceller properties of bolaform electrolytes. *J. Phys. Chem.* **1978**, *78*, 1387−90.
(23) Takiue, T.; Nakamura, F.; Murakami, D.; Fukuda, T.; Shuto, A.; Matsubara, H.; Aratono, M. Molecular orientation and multilayer formation of 1H,1H,8H,8H-perfluorooctane- 1,8-diol at the air/water interface. *J. Phys. Chem. B* **2009**, *113*, 6305−6310.
(24) Takiue, T.; Fukuda, T.; Murakami, D.; Inomata, H.; Sakamoto, H.; Matsubara, H.; Aratono, M. Molecular orientation and multilayer formation in the adorbed film of 1H,1H,10H,10H-perfluorodecane-1,10-diol at the hexane/water interface; Temperature effect on the adsorption of fluoroalkane-diol. *J. Phys. Chem. B* **2008**, *112*, 5078−5084.
(25) Takiue, T.; Fukuda, T.; Murakami, D.; Sakamoto, H.; Matsubara, H.; Aratono, M. Moleucular orientation and multilayer formation in the adsorbed film of 1H,1H,10H,10H-perfluorodecane-1,10-diol at the hexane/water interface; Pressure effect on the adsorption of fluoroalkane-diol. *J. Phys. Chem. B* **2009**, *113*, 14667−14673.
(26) Sakamoto, H.; Murao, A.; Hayami, Y. Real-time measurement of interfacial tension by image processing. *J. Inst. Image Inf. Television Eng.* **2002**, *56*, 1643−1650.
(27) Takiue, T.; Tottori, T.; Tatsuta, K.; Matsubara, H.; Tanida, H.; Nitta, K.; Uruga, T.; Aratono, M. Multilayer Formation of Fluoroalkanol − ω-Hydrogenated fluorocarbon mixture at the hexane/water interface studied by interfacial tensiometry and X-ray reflection. *J. Phys. Chem. B* **2012**, *116*, 13739−13748.
(28) Pershan, P. S. Structure of surfaces and interfaces as studied using synchrotron radiation. *Faraday Discuss. Chem. Soc.* **1990**, *89*, 231−245.
(29) Zhang, Z.; Mitrinovic, D. M.; Williams, S. M.; Huang, Z.; Schlossman, M. L. X-ray scattering from monolayer of F-$(CF_2)_{10}(CH_2)_2OH$ at the water-(hexane solution) and water vapor interfaces. *J. Phys. Chem. B* **1999**, *110*, 7421−7432.
(30) Als-Nielsen, J.; Jacquemain, D.; Kjaer, K.; Leveiller, F.; Lahav, M.; Leiserowitz, L. Principles and applications of grazing incidence X-ray and neutron scattering from ordered molecular monolayers at the air-water interface. *Phys. Rep.* **1994**, *246*, 251−313.
(31) Buff, F. P.; Lovett, R. A.; Stillinger, F. H. Interfacial density profile for fluids in the critical region. *Phys. Rev. Lett.* **1965**, *15*, 621−623.
(32) Wu, E. S.; Webb, W. W. Critical liquid-vapor interface in SF_6. 1. Thickness of the diffuse transition layer. *Phys. Rev. A* **1973**, *8*, 2065−2076.
(33) Motomura, K. Thermodynamic studies on adsorption at interfaces. 1. General formulation. *J. Colloid Interface Sci.* **1978**, *64*, 348−355.
(34) Aratono, M.; Villeneuve, M.; Takiue; Ikeda, N.; Iyota, H. Thermodynamic consideration of mixtures of surfactants in adsorbed films and micelles. *J. Colloid Interface Sci.* **1998**, *200*, 161−171.
(35) Murakami, D.; Fukuda, T.; Matsubara, H.; Aratono, M.; Takiue, T. Molecular orientation and miscibility of fluorinated α,ω-alkanediol and alcohol at the hexane/water interface. *Colloids Surf., A* **2010**, *354*, 205−209.
(36) Aratono, M.; Murakami, D.; Matsubara, H.; Takiue, T. Phase transition and domain formation in the Gibbs adsorbed films of long-chain alcohols. *J. Phys. Chem. B* **2009**, *113*, 6347−6352.